Polymer 50 (2009) 541–546

Contents lists available at ScienceDirect

Polymer

journal homepage: www.elsevier.com/locate/polymer

Interaction of nanogel with cyclodextrin or protein: Study by dynamic light scattering and small-angle neutron scattering

Norihiro Inomoto [a], Noboru Osaka [a], Takuya Suzuki [a], Urara Hasegawa [b], Yayoi Ozawa [b], Hitoshi Endo [a], Kazunari Akiyoshi [b], Mitsuhiro Shibayama [a,*]

[a] Institute for Solid State Physics, The University of Tokyo, 5-1-5 Kashiwanoha, Kashiwa, Chiba 277-8581, Japan
[b] Institute of Biomaterials and Bioengineering, Tokyo Medical and Dental University, 2-3-10 Kanda-Surugadai, Chiyoda-ku, Tokyo 101-0062, Japan

ARTICLE INFO

Article history:
Received 27 March 2008
Received in revised form
12 October 2008
Accepted 3 November 2008
Available online 8 November 2008

Keywords:
Nanogel
Molecular chaperon
Pullulan

ABSTRACT

The structure of hydrogel nanoparticles (CHP nanogels), formed by self-aggregation of cholesterol-bearing pullulan (CHP) was studied by dynamic light scattering (DLS) and small-angle neutron scattering (SANS). The interactions between the CHP nanogel and methyl-β-cyclodextrin (CD) or protein (hen egg white) were also investigated. It was revealed by SANS that the nanogels were spherical in shape with a radius of 6.7 nm. The following two functions were disclosed. (1) CHP nanogels were dissociated by the addition of CD and formed inclusion complexes with cholesteryl groups, leading to suppression of hydrophobic interaction between the cholesteryl groups. (2) The nanogel behaved as a molecular chaperone (heat shock protein-like activity) when CHP nanogel was mixed with hen egg white and heated up to 75 °C. The egg white aqueous solutions with CHP nanogel remained transparent while the egg white without CHP nanogel became opaque.

1. Introduction

Molecular chaperones, which stabilize the correct folding of a protein, have attracted much attention because of the ability to recover the function lost by denaturation [1,2]. Molecular chaperones are originally defined as a group of proteins that help proper assembling of other proteins, but are not themselves components of the final functional structures [3]. It is suggested that neurodegenerative diseases, such as Prion disease, Alzheimer's disease and Parkinson's disease, have happened owing to misfolding or aggregation of proteins [4,5]. From the viewpoint of a medical treatment, prevention of protein aggregation is significant. Therefore, a molecular chaperone is expected to be a candidate for curing neurodegenerative diseases. For example, it was reported that the endoplasmic reticulum chaperone suppressed the formation of beta amyloid fiber which causes Alzheimer disease [6,7]. Molecular chaperones selectively trap intermediate proteins (folding intermediate or partially denatured proteins under heating) to prevent irreversible aggregation due to macromolecular host (molecular chaperone)–guest (protein) interactions. With the aid of ATP and another co-chaperone, the host chaperone then releases the protein in its refolded form.

Many studies have been done to create artificial molecular chaperones to mimic these functions of chaperones since the last decade [8,9]. Akiyoshi et al. have attempted to design artificial molecular chaperone systems using self-assembled nanogels [10]. We have reported that nanometer-sized (20–30 nm) polymer hydrogels were formed by self-aggregation of hydrophobized polysaccharides such as cholesterol-bearing pullulan (CHP nanogels, Fig. 1) [10]. The main driving force for self-aggregation is hydrophobic association between the cholesteryl groups in water.

Several interesting properties have been studied about the CHP nanogels as schematically illustrated in Fig. 2. (1) Dissociation of the CHP nanogel has been observed by addition of methyl-β-cyclodextrin (CD), which eliminated hydrophobic interaction between cholesteryl groups [11–13]. It is reported that CD acts as a suitable host of the various hydrophobic compounds because of strong hydrophobicity of the cavity of a CD molecule [14–16]. As a matter of fact, Breslow et al. have reported that CD binds cholesteryl groups into its cavity as a host–guest interaction [17]. (2) The CHP nanogels were capable of trapping proteins, e.g., bovine serum albumin (BSA) inside the CHP nanogel [18–23]. Previously, we investigated heat shock protein-like activity (thermal stabilization) for enzymes such as carbonic anhydrase by an artificial molecular chaperone (CHP nanogel–cyclodextrin system) [13,22]. This system involves a two-step mechanism. CHP nanogels prevent protein aggregations upon heating by complexation with denatured proteins. The dynamics of molecular chaperones is controlled by

* Corresponding author.
E-mail address: shibayama@issp.u-tokyo.ac.jp (M. Shibayama).

0032-3861/$ – see front matter © 2008 Published by Elsevier Ltd.
doi:10.1016/j.polymer.2008.11.001

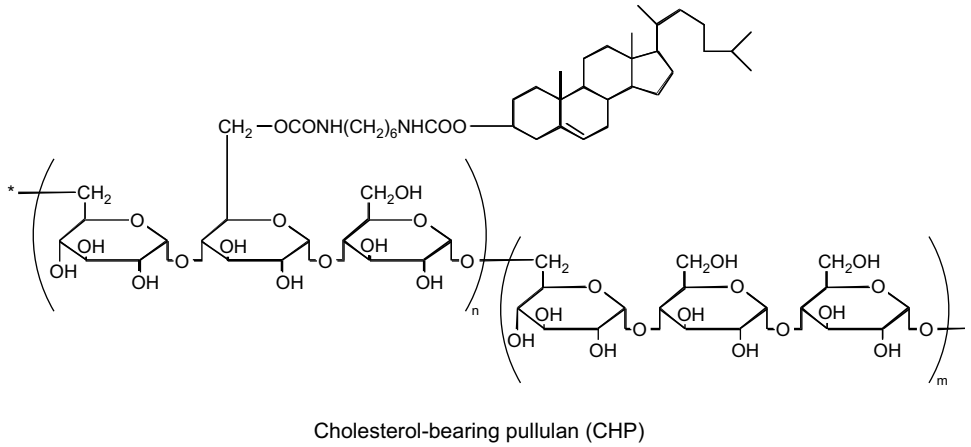

Cholesterol-bearing pullulan (CHP)

Fig. 1. Structure of cholesterol-bearing pullulan (CHP).

the binding of suitable effectors such as ATP and co-chaperone. In our artificial system, CDs were used as modulators of the structure of nanogels. The dissociation of the nanogel by the addition of CD caused an attenuation of the interaction between the nanogel and the denatured protein. Thus, protein folding is predicted to start under the more hydrophilic environment.

As mentioned above, many studies about molecular chaperone have been done by using macroscopic measurements. However, only a few workers have studied molecular chaperone from viewpoint of microscopic structure change in detail. The aim of this work is to examine the validity of this model and to carry out more sophisticated structural analyses, i.e. (i) the structure of the CHP nanogel, (ii) the interaction of the CHP nanogel with CD, and (iii) the interaction of the CHP nanogel with white hen egg under heating as a model of biomimetic molecular chaperone (heat shock protein-like activity), by dynamic light scattering (DLS) and small-angle neutron scattering (SANS).

2. Experimental section

2.1. Materials

Cholesterol-bearing pullulan (CHP), which was substituted with 1.4 cholesteryl groups per 100 glucose units of the pullulan ($M_w = 1.0 \times 10^5$), was prepared as previously reported [10]. CHP was suspended in phosphate buffered saline (PBS, pH 7.4) at 70 °C for 2 h. The suspension was filtered (Millex-GS; $\phi = 0.8$ mm; Millipore) and sonicated for 15 min at 25 °C with a sonicator probe (Branson Sonifier 250) operated at 40 W. The solution was further filtered through Millex-GS filter ($\phi = 0.22$ μm; Millipore) for measurement of SANS. In the case of DLS measurement, the solution was centrifuged at 19,280*g* for 30 min and half of the supernatant solution was skimmed. Methyl-β-cyclodextrin (CD) was purchased from Tokyo Kasei Kogyo Co., Ltd. The egg white was commercially available. All the samples were eluted by PBS (pH 7.4). The concentration of the samples was as follows: the CHP nanogel was 0.50–20 mg/mL (1.1–44 μM), CD was 4.8×10^{-3}–2.4×10^{-1} mg/mL (3.7–180 μM). Deuterated water was used for preparation of each solution in order to obtain scattering contrast for small-angle neutron scattering. It has been reported that the CHP nanogels are able to form stronger complexes with heat-denatured proteins than native proteins as molecular chaperones [23]. The mixture of the proteins and the CHP nanogels was heated at 75 °C which is above the denaturation temperature of the proteins for 5 min., and it was cooled down to 25 °C for the measurements.

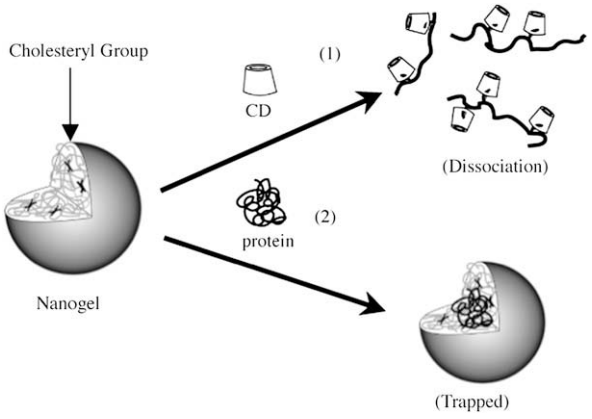

Fig. 2. Schematic representation of assembling CHP nanogel with protein and CD suggested from the previous literatures [11–23].

2.2. Dynamic light scattering (DLS)

DLS measurements were performed by a static/dynamic compact goniometer (DLS/SLS-5000), ALV, Langen, Germany. A He–Ne laser with a power of 22 mW emitting a polarized light at $\lambda = 6328$ Å was used as the incident beam. DLS measurements were taken at 25 °C at several angles including 90°. In a DLS measurement, we obtain the intensity–intensity–time correlation function, $g^{(2)}(\tau)$, which is linked to the scattered electric field correlation function, $g^{(1)}(\tau)$,

$$g^{(2)}(\tau) = 1 + \beta\left|g^{(1)}(\tau)^2\right| \quad (1)$$

where τ is the decay time and β is the instrumental coherence factor close to unity [24]. $g^{(1)}(\tau)$ is described by the decay rate distribution function, $G(\Gamma)$,

$$g^{(1)}(\tau) = \int_0^\infty G(\Gamma)\exp(-\Gamma\tau)\mathrm{d}\Gamma \quad (2)$$

where Γ is the relaxation rate. $G(\Gamma)$ was calculated from Laplace inversion of $g^{(2)}(\tau)$ on the basis of Eqs. (1) and (2) [24]. In this study, the CONTIN (constrained regularization method) [25] program supplied with the correlator was used to obtain $G(\Gamma)$ from $g^{(2)}(\tau)$.

2.3. Small-angle neutron scattering (SANS)

SANS experiments were carried out at the SANS instrument (SANS-U) of Institute for Solid State Physics, the University of Tokyo [26]. The neutron wavelength was 7.0 Å, and its distribution was ca.

10%. The sample-to-detector distance was chosen to be 2 and 8 m. The necessary corrections were made, such as air scattering, cell scattering, and incoherent background subtraction. After these corrections, the scattered intensity was normalized to the absolute intensity in terms of the scattering intensity from a standard sample [26]. The temperature of the samples was regulated to be 25 °C.

3. Results and discussion

3.1. Characterization of CHP nanogel

Fig. 3a shows a typical decay rate distribution function of the DLS results among 50 measurements of the CHP nanogel (0.5 mg/mL) at a scattering angle of 90°. As shown in this figure, this system has a unimodal distribution ($\Gamma^{-1} \approx 0.2$ ms). To examine the origin of these modes, q-dependent DLS measurements were carried out. When a relaxation mode is diffusive, its relaxation decay rate, Γ, obeys the following equation,

$$D = \frac{\Gamma}{q^2} \tag{3}$$

where the D is the diffusion constant [24]. Fig. 3b shows the q dependence of the decay rate for a unimodal distribution mode at $T = 25$ °C, where $q = (4\pi n_0/\lambda)\sin(\theta/2)$ is the magnitude of scattering vector, with the wavelength, λ, the refractive index of the solvent, n_0, and the scattering angle, θ. As shown here, the relaxation mode clearly shows q^2 dependence of Γ, confirming that the relaxation motion is diffusive. The hydrodynamic radius, R_h, can be obtained by the Stokes–Einstein equation:

$$R_h = \frac{kT}{6\pi\eta D} \tag{4}$$

where η is the viscosity of the solvent, k is the Boltzmann constant, and T is the absolute temperature. The diffusion constant, D, was obtained as the slope of the line in Fig. 3b. The value of D was estimated to be 2.47×10^{-11} m^2/s which corresponds to $R_h = 10.0$ nm. It should be noted that the molecular weight of the pullulan used is 1.0×10^5 g/mol, and based on the previous study, the aggregation number is ~4.2 [27]. This leads to the estimation that effective molecular weight of the aggregate is about 4.2×10^5. Therefore, the obtained R_h value seems to be less than the above expected value. This disparity is due to the fact that the pullulan chains are folded by the cholesteryl groups. We can conclude that the estimated value is in good agreement with the previous work, which suggests that the mode stems from translational diffusion of the CHP nanogel [10,27].

Fig. 4a shows the SANS intensities, $I(q)$'s for pullulan (open circles) and the CHP nanogel (filled circles). First of all, let us discuss the scattering function of pullulan. Since a pullulan is a flexible chain [28] and have little hydrophobic interaction without the cholesteryl groups, we fitted the scattering profile of pullulan by Debye function,

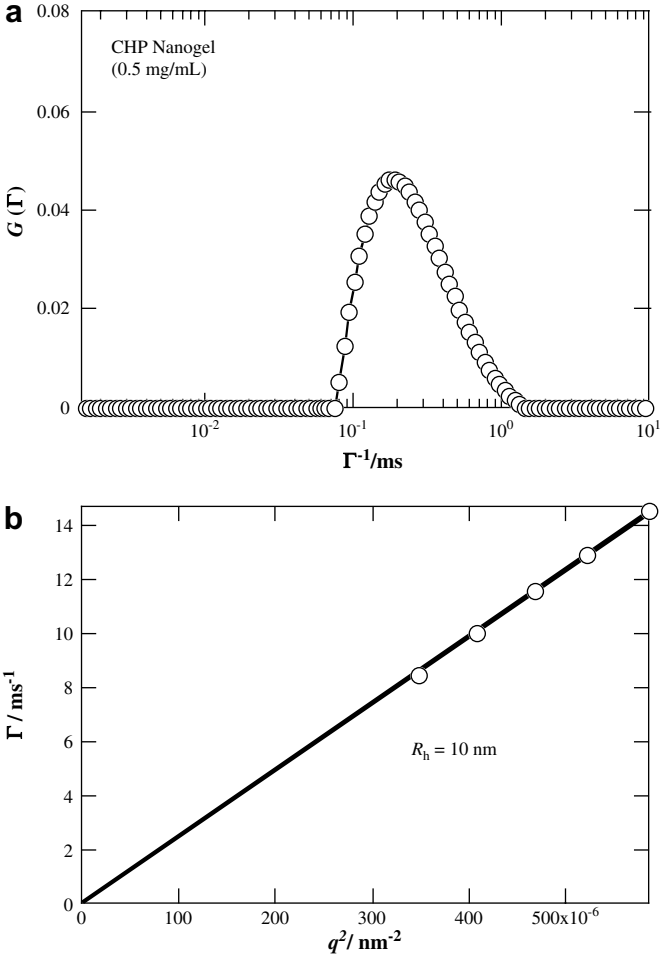

Fig. 3. (a) A typical decay rate distribution function obtained by the DLS measurements at a fixed angle of 90° for CHP nanogels. (b) The decay rate, Γ, vs q^2 plots.

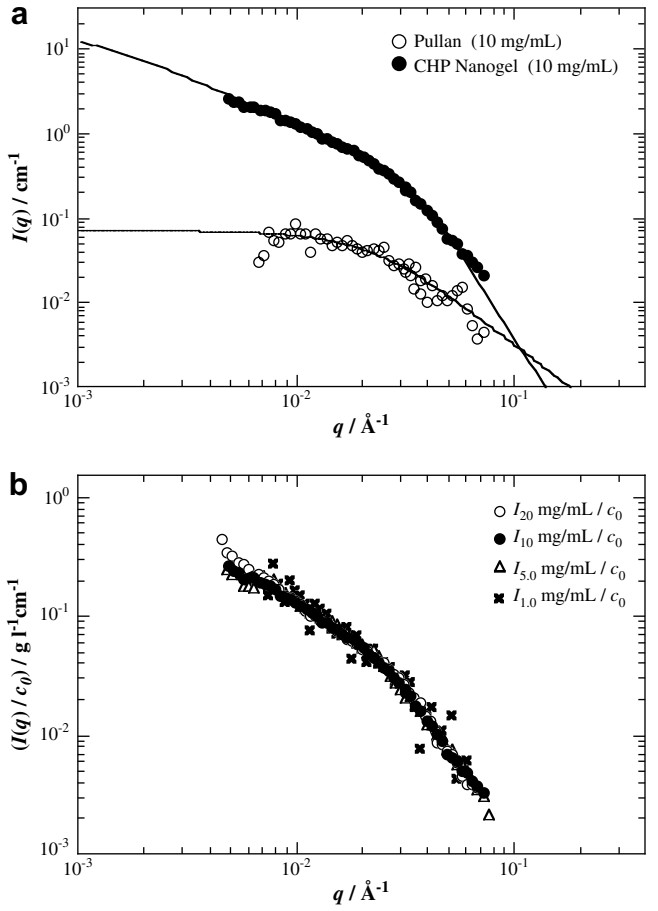

Fig. 4. (a) SANS results of CHP nanogel and pullulan. Fitting curves of CHP nanogel and pullulan are also shown. (b) Reduced SANS intensity curves with CHP concentration, c_0 (= 10 mg/mL), for CHP nanogel (20 mg/mL), CHP nanogel (10 mg/mL), CHP nanogel (5.0 mg/mL), and CHP nanogel (1.0 mg/mL).

$$P(q) = 2\frac{\exp\left(-q^2R_g^2\right) + q^2R_g^2 - 1}{\left(q^2R_g^2\right)^2} \quad (5)$$

where R_g is the radius of gyration. The R_g was estimated to be 6.6 nm.

$I(q)$ of the CHP nanogel is much higher than that of pullulan, which indicates that self-assembled aggregates (CHP nanogels) were certainly formed. Next, let us discuss the fitting of the scattering curves. In principle, $I(q)$ is expected to be a product of both contributions from the form factor $P(q)$ and the structure factor $S(q)$ given by:

$$I(q) = nV^2\Delta\rho^2P(q)S(q) \quad (6)$$

where n is the number density of the sphere, $\Delta\rho^2$ is the square of the difference between the scattering length densities of the particle and the solvent. The form factor for a sphere, $P(q)$, is given by:

$$P(q) = \Phi^2(qR) \quad (7)$$

$$\Phi(qR) = \frac{3[\sin(qR) - qR\cos(qR)]}{(qR)^3} \quad (8)$$

Here, the deviation, ΔR, of the radius of the sphere was included as a Gaussian function [29].

As is shown in the scattering curves, an upturn at low q region is observed, which suggests the presence of interparticle interactions. We previously reported that in semidilute solution above approximately 25 mg/mL, the viscosity of the CHP nanogel solution drastically increased. At higher concentration, they formed macroscopic gel: CHP gave a structure in which the nanoparticles are linked [27]. Hence, we introduced the effect of fractal aggregation as the intermolecular correlation, $S(q)$. The $S(q)$ is given by the Freltoft–Kjems–Sinha function as follows [30]:

$$S(q) = 1 + \frac{C\left(d_f - 1\right)\Gamma\left(d_f - 1\right)\xi^{d_f}}{\left(1 + q^2\xi^2\right)^{d_f/2}} \frac{\left(1 + q^2\xi^2\right)^{1/2}}{q\xi} \times \frac{\sin\left[\left(d_f - 1\right)\arctan(q\xi)\right]}{d_f - 1} \quad (9)$$

where ξ is the size of fractal aggregates, C is a constant, and d_f is the fractal dimension. The fitting curve (solid line) well reproduced the scattering curves as shown in Fig. 4a. The R of the CHP nanogel was estimated to be 6.7 nm with $\Delta R = 1.5$ nm. The ξ and d_f were obtained to be 114 nm and 1.36, respectively.

Fig. 4b shows the scattering curves of CHP nanogels which are normalized by the concentration, c_0 ($= 10$ mg/mL). Each normalized scattering curve is nicely superimposed to a single master curve with $\xi = 114$ nm and $d_f = 1.36$. This indicates that CHP nanogels have similar structure irrespective of the concentrations investigated in this work (1.0–20 mg/mL).

3.2. Interaction of CHP nanogel with CD

It is well known that CD acts as a good host of the hydrophobic groups (e.g., cholesteryl groups) due to the strong hydrophobicity of the cavity of a CD molecule [15,17] When CHP nanogel is mixed with CD, the cholesteryl group of a CHP nanogel is expected to thread into CD molecule. As Akiyoshi et al. reported, it was suggested by high-performance size exclusion chromatography (HPSEC) that the CHP nanogel was dissociated by addition of CD [11]. Hence, CD is anticipated to suppress the hydrophobic interactions between the cholesteryl groups in the CHP nanogel, resulting in the dissociation of nanogel [11,13]. We prepared 10 mg/mL CHP nanogel solution and gradually added CD into the solution.

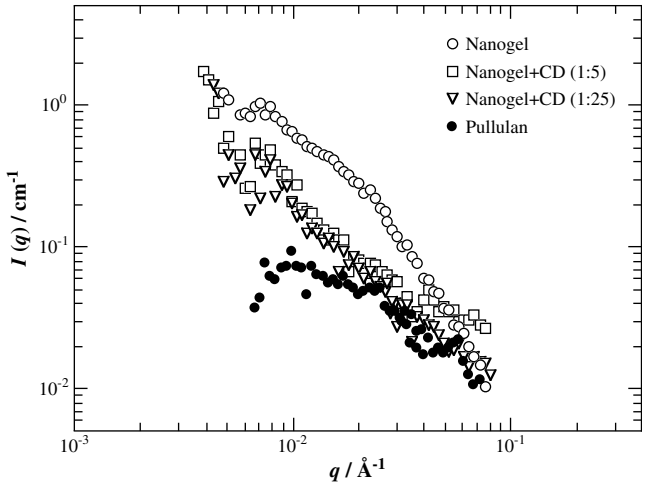

Fig. 5. SANS intensity curves for CHP nanogel (○), CHP nanogel+ CD (5 equiv., □), CHP nanogel + CD (25 equiv., ▽) and pullulan. (●).

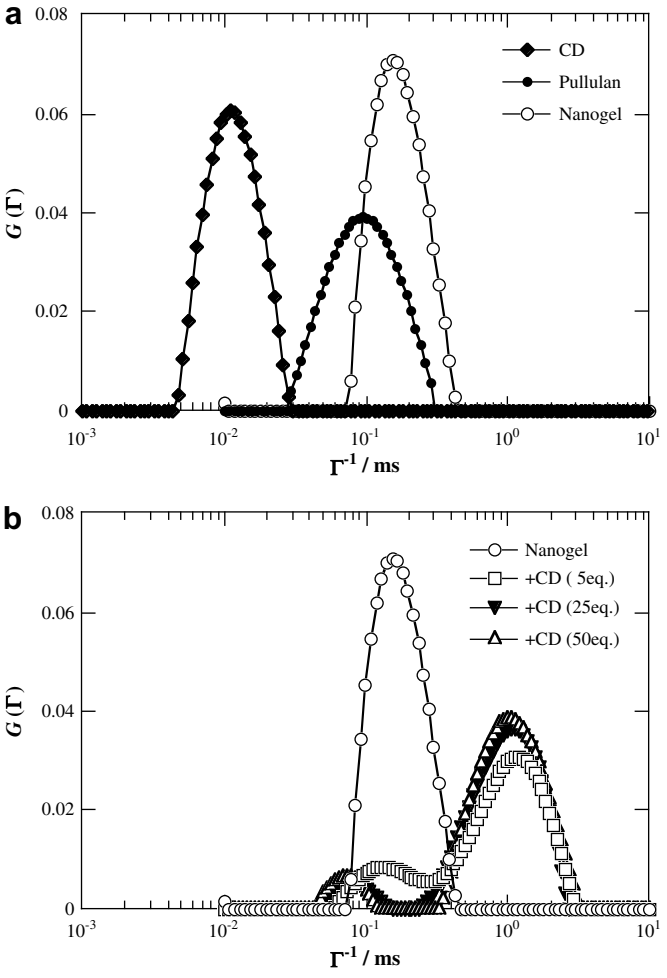

Fig. 6. (a) Decay rate distribution functions obtained by the DLS measurements at a fixed angle of 90° for (a) CD (◆), Pullulan (●), and CHP nanogel (○), and (b) CHP nanogel (○), CHP nanogel + CD (5 equiv., □), CHP nanogel + CD (25 equiv., ▼) and CHP nanogel + CD (50 equiv., △).

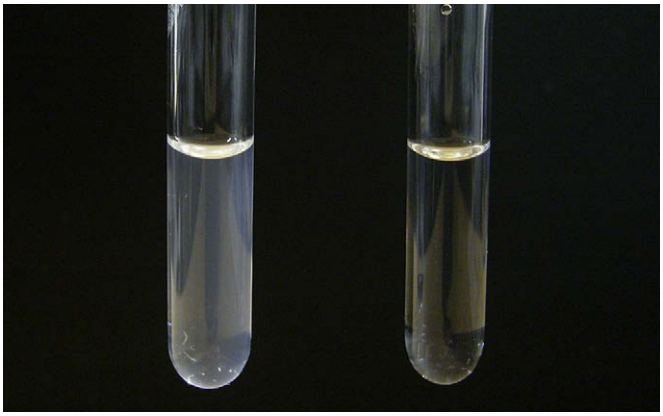

Fig. 7. Photograph showing hen egg white aqueous solutions without (left) or with (right) CHP nanogel (1.0 mg/mL). Egg white was diluted 300-fold by adding buffer (PBS, pH 7.4). Both solutions were incubated at 75 °C for 5 min.

The amount of CD was 5 eq./25 eq. to the cholesteryl groups in the CHP nanogel.

Fig. 5 shows SANS profiles of the CHP nanogel, pullulan, and mixtures of CHP nanogel and CD. As shown in the figure, the scattering intensity of the CHP nanogel decreased as the concentration of CD increased. It is considered that the CHP nanogels were certainly dissociated by an addition of CD. At the high q region, the scattering intensities were almost the same as that of pullulan, which indicates that the CHP nanogels were dissociated to be the flexible-chain-like structure as discussed above. On the other hand, an upturn of the scattering intensities is observed at the low q region. This upturn indicates that certain amount of aggregates exist simultaneously with the generation of the pullulan-like structure.

Fig. 6a shows the decay rate distribution functions for CD, pullulan and the CHP nanogel obtained by the DLS measurements at a fixed angle of 90°. The CHP nanogel shows a single peak ($\Gamma^{-1} \approx 0.2$ ms) at the relaxation time slower than that of pullulan ($\Gamma^{-1} \approx 0.1$ ms). Fig. 6b shows the DLS results for the mixtures of the CHP nanogel and CD (5–50 eq. to the cholesterol groups) obtained by the DLS measurements at a fixed angle of 90°. As shown in the figure, the following findings were obtained: (1) when CD was added to CHP nanogel, the peak of CHP nanogel was suppressed. (2) The more CD was added, the more Γ^{-1} of the peak originating from the CHP nanogel shifted to the faster decay time ($\Gamma^{-1} \approx 0.1$ ms, Fig. 6b). (3) On the other hand, a new peak appeared in the slower decay time ($\Gamma^{-1} \approx 1$ ms).

The findings (1) and (2) indicate that CHP nanogel is dissociated by the addition of CD. Particularly, (2) implies that CD destroys the hydrophobic association, leading to a dissociation of nanogel to a random coil-like chains like pullulan ($\Gamma^{-1} \approx 0.1$ ms). On the other hand, however, (3) suggests a generation of larger aggregates as

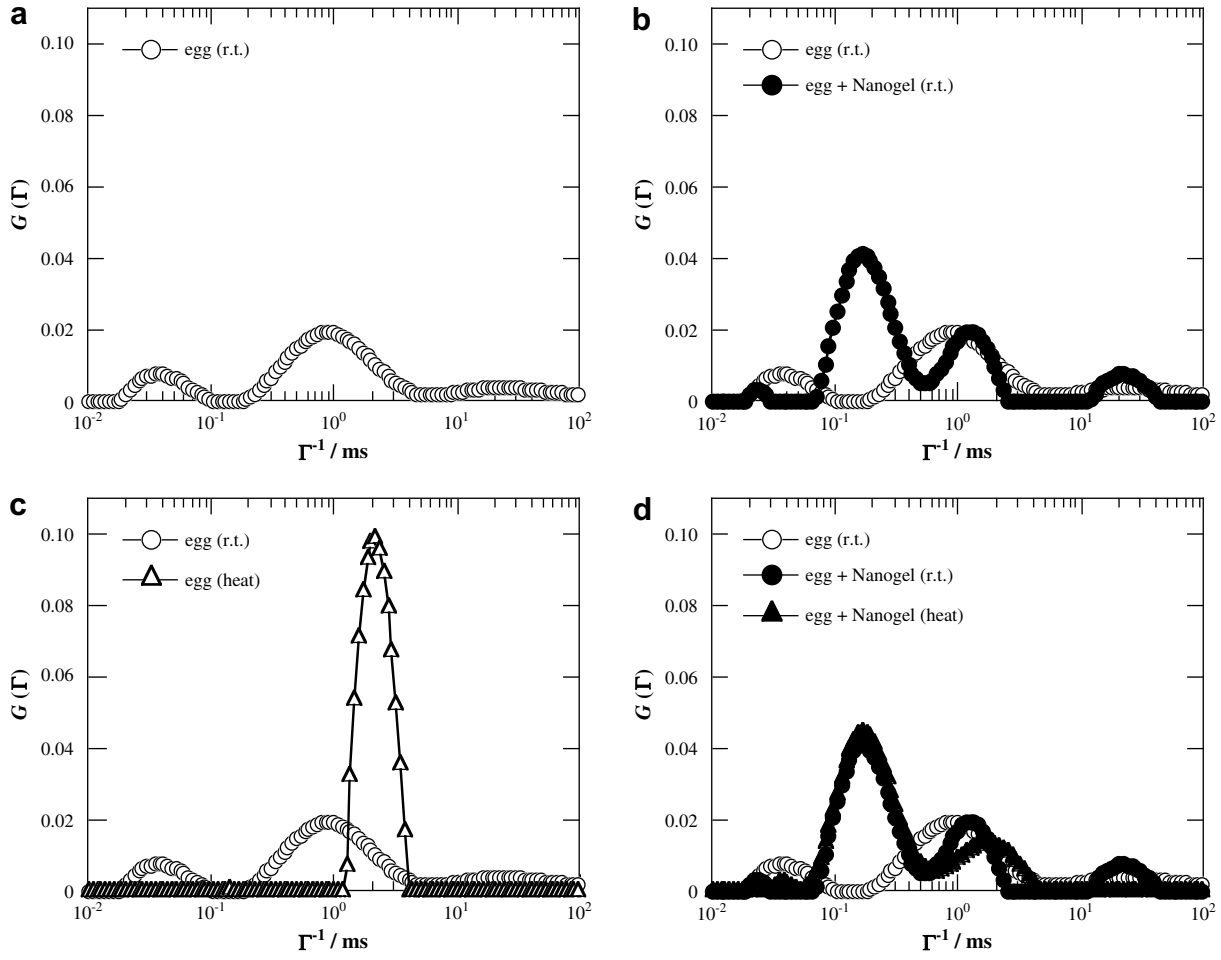

Fig. 8. Decay rate distribution functions obtained by the DLS measurements at a scattering angle of 90° for hen egg white (r.t. (a) or heated (b)), and hen egg white + CHP nanogel (r.t. (c) or heated (d)).

well. It may indicate that some of the dissociated CHP chains are bonded via cholesterol units, forming a larger coagulates. This new result is consistent with the SANS result shown in Fig. 5.

3.3. Interaction of CHP nanogel with hen egg white

In order to observe heat shock protein-like activity of molecular chaperone, let us show the result of a simple demonstration using hen egg white and the CHP nanogel in Fig. 7. The egg white was diluted by 300-fold by phosphate buffered saline (PBS, pH 7.4) as previously reported by Taguchi [31]. Two samples were prepared without and with the CHP nanogels. After heating the solutions at 75 °C for 5 min, changes of the solutions were visually observed. The solution without nanogels became opaque as a result of heat-induced denaturation of protein followed by aggregation, whereas the solution with nanogels remained transparent. This observation clearly indicates that CHP nanogel prevents the egg white from aggregation. We investigated this phenomenon in detail by DLS at scattering angle 90°. Fig. 8 shows $G(\Gamma)$s of egg white solutions. When the egg white was first measured at room temperature (25 °C), a broad distribution curve with two broad peaks was observed (see Fig. 8a). These peaks can be assigned to ovalbumin and other proteins [32]. When the solution was heated at 75 °C for 5 min, a new peak appeared around $\Gamma^{-1} \approx 2$ ms ($R_h = 180$ nm) (Fig. 8b). It can be conjectured that this peak represents heat-denatured aggregates of an egg white. On the other hand, $G(\Gamma)$ of the egg white solution containing CHP nanogel remained unchanged by heating (Fig. 8c and d). This result clearly indicates that the CHP nanogel has suppressed a heat-induced denaturation of egg white by interaction with heat-denatured egg white. This behavior is similar to the function of molecular chaperon GroEL [31].

4. Conclusion

The structural properties of CHP nanogels and the interaction of CHP nanogel with CD, or its chaperone-like function, were investigated in detail SANS and DLS. The following conclusions were drawn by DLS analysis and SANS curve fitting. (1) The core and the hydrodynamic radii of the CHP nanogel were determined to be 6.7 nm and 10.0 nm, respectively. (2) The ξ and d_f were obtained to be 114 nm and 1.36, respectively. (3) The SANS intensity of the CHP nanogel decreased as the concentration of CD increased. This indicates that the CHP nanogels are dissociated by an addition of CD. (5) The CHP nanogel was partially destroyed by CD while larger clusters were also formed via associating cholesteryl groups. (6) In addition, the chaperone-like function of the CHP nanogel was observed by DLS. In the presence of the CHP nanogel, the R_h of the mixture of egg white and CHP nanogel did not change by heating, which demonstrates the activity of the CHP nanogel as a molecular chaperone.

Acknowledgement

This work was also partially supported by the Ministry of Education, Science, Sports and Culture, Japan (Grant-in-Aid for Scientific Research (A), 2006–2008, No. 18205025, and for Scientific Research on Priority Areas, 2006–2010, No. 18068004). The SANS experiment was performed with the approval of Institute for Solid State Physics, The University of Tokyo (Proposal Nos. 06.237), at Japan Atomic Energy Agency, Tokai, Japan.

References

[1] Ellis RJ. Trends Biochem Sci 1998;23:43–5.
[2] Guise AD, West SM, Chaudhuri JB. Mol Biotechnol 1996;6:53–64.
[3] Ellis J. Nature 1987;328:378–9.
[4] Minghetti L. Curr Opin Neurol 2005;18:315–21.
[5] Castellani RJ, Perry G, Smith MA. Acta Neurobiol Exp 2004;64:11–7.
[6] Hoshino T, Tsutsumi S, Tomisato W, Hwang HJ, Tsuchiya T, Mizushima T. J Biol Chem 2003:278.
[7] Hoshino T, Nakaya T, Araki W, Suzuki K, Suzuki T, Mizushima T. Biochem J 2007; 402:581–9.
[8] Rariy RV, Klibanov AM. Proc Natl Acad Sci U S A 1997:94.
[9] Hanson PE, Gellman SH. Fold Des 1998;3:457–68.
[10] Akiyoshi K, Deguchi S, Moriguchi N, Yamaguchi S, Sunamoto J. Macromolecules 1993;26:3062–8.
[11] Akiyoshi K, Sasaki Y, Kuroda K, Sunamoto J. Chem Lett 1998;27:93–4.
[12] Akiyoshi K, Ueminami A, Kurumada S, Nomura Y. Macromolecules 2000;33: 6752–6.
[13] Nomura Y, Sasaki Y, Takagi M, Narita T, Aoyama Y, Akiyoshi K. Biomacromolecules 2005;6:447–52.
[14] Shiotani K, Uehara K, Irie T, Uekama K, Thompson DO, Stella VJ. Pharmacol Res 1995;12:78–84.
[15] Yang Z, Breslow R. Tetrahedron Lett 1997;38:6171–2.
[16] Mucci A, Vandelli MA, Salvioli G, Malmusi L, Forni F, Schenetti L. Supramol Chem 1996;7:125.
[17] Breslow R, Zhang B. J Am Chem Soc 1996;118:8495–6.
[18] Nishikawa T, Akiyoshi K, Sunamoto J. Macromolecules 1994;27:7654–9.
[19] Nishikawa T, Akiyoshi K, Sunamoto J. J Am Chem Soc 1996;118:6110–5.
[20] Akiyoshi K, Kobayashi S, Shichibe S, Mix D, Baudys M, Kim SW, et al. J Controlled Release 1998;54:313–20.
[21] Akiyoshi K, Sunamoto J. Supramol Sci 1996;3:157–63.
[22] Akiyoshi K, Sasaki Y, Sunamoto J. Bioconjugate Chem 1999:10.
[23] Nomura Y, Ikedaa M, Yamaguchi N, Aoyama Y, Akiyoshi K. FEBS Lett 2003; 553:271–6.
[24] Brown W. Dynamic light scattering, the methods and applications. Oxford: Clarendon Press; 1993.
[25] Provencher SW. Comput Phys Commun 1982;27:213–27.
[26] Okabe S, Nagao M, Karino T, Watanabe S, Adachi T, Shimizu H, et al. J Appl Crystallogr 2005;38:1035–7.
[27] Kuroda K, Fujimoto K, Sunamoto J, Akiyoshi K. Langmuir 2002;18:3780–6.
[28] Muroga Y, Yamada Y, Noda I, Nagasawa M. Macromolecules 1987;20:3003–6.
[29] Fuse C, Okabe S, Sugihara S, Aoshima S, Shibayama M. Macromolecules 2004; 37(20):7791–8.
[30] Freltoft T, Kjems JK, Sinha SK. Phys Rev B 1986;33:269–75.
[31] Taguchi H. J Biochem 2005;137:543–9.
[32] Stadelman WJ, Cotterill OJ. Egg science and technology. In: AVI Publishing Co; 1986.